

Radiation effects in single-walled carbon nanotube papers

Cory D. Cress,^{1,a)} Christopher M. Schauerma,² Brian J. Landi,^{2,3} Scott R. Messenger,¹ Ryne P. Raffaele,² and Robert J. Walters¹

¹Electronics Science and Technology Division, U.S. Naval Research Laboratory, Washington, DC 20375, USA

²NanoPower Research Laboratories, Rochester Institute of Technology, Rochester, New York 14623, USA

³Department of Chemical and Biomedical Engineering, Rochester Institute of Technology, Rochester, New York 14623, USA

(Received 18 August 2009; accepted 3 November 2009; published online 11 January 2010)

The effects of ionizing radiation on the temperature-dependent conductivity of single-walled carbon nanotube (SWCNT) papers have been investigated *in situ* in a high vacuum environment. Irradiation of the SWCNT papers with 4.2 MeV alpha particles results in a steady decrease in the SWCNT paper conductivity, resulting in a 25% reduction in room temperature conductivity after a fluence of 3×10^{12} alpha particles/cm². The radiation-induced temperature-dependent conductivity modification indicates that radiation damage causes an increase in the effective activation barrier for tunneling-like conductivity and a concomitant increase in wavefunction localization of charge carriers within individual SWCNTs. The spatial defect generation within the SWCNT paper was modeled and confirms that a uniform displacement damage dose was imparted to the paper. This allows the damage coefficient (i.e., differential change in conductivity with fluence) for alpha particles, carbon ions, and protons to be compared with the corresponding nonionizing energy loss (NIEL) of the incident particle. The resulting nonlinear relationship with NIEL between these parameters is distinct from the more typical linear response observed in many bulk semiconductors and superconductors and indicates that localized radiation damage in the SWCNT papers has a greater impact than distributed damage. Although SWCNT papers behave largely as a bulk material with properties that are a convolution of the underlying SWCNT distribution, the radiation response appears to be largely dominated by degradation in the preferred one-dimensional conduction within these two-dimensionally confined nanostructures. © 2010 American Institute of Physics.

[doi:10.1063/1.3268470]

I. INTRODUCTION

Single-walled carbon nanotubes (SWCNTs) are under investigation for use in a wide range of applications, such as field effect transistors,¹ transparent conductive coatings,² and gas sensors,³ in an attempt to capitalize on their superior electronic and structural properties. The effects of high-energy electron and ion irradiation on the SWCNT materials have been under study both from a reliability standpoint for devices potentially employed in radiation environments and as a practical means to tailor their structural and electronic properties.⁴

Changes in the electrical and morphological properties of carbon nanotubes (CNTs) have been investigated at the individual multiwalled CNT or SWCNT/bundle level as a function of exposure to various forms of ionizing radiation including high-energy photons,⁵ electrons,⁶ protons,⁷ and ions.^{8,9} The changes observed in electrical conductivity are the result of an electron- or ion-induced displacement of a carbon atom, leading to point vacancies, divacancies, carbon adatoms, and other defect structures that disrupt the electronic structure.⁴ Measurements of isolated CNTs or SWCNT bundles post-irradiation indicate that radiation exposure causes a reduction in the electrical conductivity of the

materials, although, at low defect levels (low doses), inter-shell bridging between neighboring CNTs may improve the inter-CNT conductivity and has been suggested as a mechanism explaining the observed increase in conductivity at the macroscopic SWCNT bundle scale.^{10,11}

In the present study, the effects of alpha-particle irradiation on high-purity freestanding SWCNTs papers are investigated. In paper form, the electrical properties of SWCNT materials may be dramatically different from those of individual SWCNTs or SWCNT bundles. This stems from the presence of both semiconducting and metallic SWCNTs, and the network of randomly aligned SWCNTs forming many possible percolation pathways, but requiring electron transport between neighboring SWCNTs and SWCNT bundles, which may have higher tunneling barriers.¹² These characteristics lead to a temperature-dependent conductivity that may resemble either metallic, semiconducting, or an ensemble response, depending on the sample components. As a result, the temperature dependence can be used to assess the nature of the dominant conduction mechanisms in the SWCNT papers and can also be used to monitor the radiation-induced changes therein.

II. EXPERIMENTAL

To avoid the effects of gas adsorption on the resulting radiation response of the SWCNTs, 4.2 MeV alpha particle

^{a)}Author to whom correspondence should be addressed. Electronic mail: cory.cress@nrl.navy.mil.

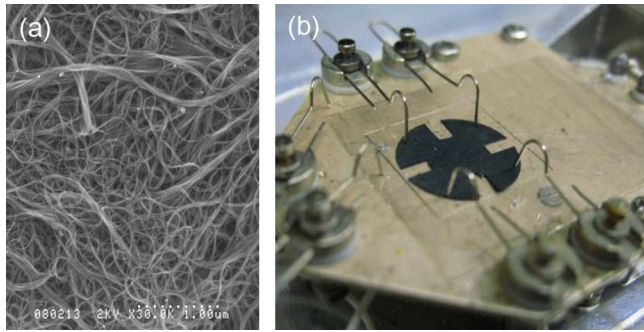


FIG. 1. (Color online) (a) A representative SEM image of high-purity laser SWCNTs used to fabricate SWCNT papers and (b) a digital photograph illustrating the SWCNT paper cloverleaf geometry and stage for temperature-dependent measurements.

irradiation of the papers was performed *in vacuo* at a pressure of $<5 \times 10^{-6}$ Torr. Laser-synthesized SWCNTs were produced and purified to $>99\%$ relative purity following previously reported procedures.^{13,14} The high purity of the sample was qualitatively investigated using a Hitachi S-900 field emission scanning electron microscope (SEM) operated at 2 keV. A representative SEM image of the purified SWCNT material is provided in Fig. 1(a). A 35 μm thick SWCNT paper was subsequently prepared via vacuum filtration (1 μm polytetrafluoroethylene-PTFE filter paper) of a solution of resuspended purified SWCNTs in *N,N*-dimethylacetamide, followed by drying in air at 250 $^{\circ}\text{C}$ for 1 h to remove the residual solvent. The temperature-dependent electrical characterization was conducted *in situ* using an Accent Technologies four-point probe station with an HL5550 LN₂ cryostat over the temperature range of 150–400 K. High-purity SWCNT papers cut into cloverleaf geometries were used in all conductivity measurements. A digital photograph of the SWCNT paper resting on the cryostat stage is provided in Fig. 1(b). Alpha-particle radiation was emitted isotropically from a 1 mCi ²¹⁰Po radioisotope foil source held approximately 14 mm from the SWCNT paper within the cryostat. Alpha particles are emitted through a thin Ni–Au coating; MCNPX simulations of the source foil indicate that the alpha-particle emission spectrum is heavy tailed (on the low energy side) with a peak energy of 4.18 MeV and a full width at half maximum of 0.21 MeV.

III. EXPERIMENTAL RESULTS

The effects of alpha particle irradiation on the temperature-dependent conductivity of a high-purity SWCNT paper are shown in Fig. 2(a). Prior to irradiation, the conductivity of the SWCNT paper is nearly constant with temperature, varying by $\pm 8\%$ from the 300 K conductivity value at the two temperature extremes. Throughout the temperature range of 150–350 K, a steady increase in conductivity is observed and is a characteristic of fluctuation assisted tunneling between neighboring SWCNTs and SWCNT bundles.¹² For this type of conduction to dominate, the energy on either side of the barrier (in this case the vacuum barrier) must be identically positioned, the appropriate wavefunction overlap is required, and the sites on either side of the barrier must be sufficiently large to eliminate electrical

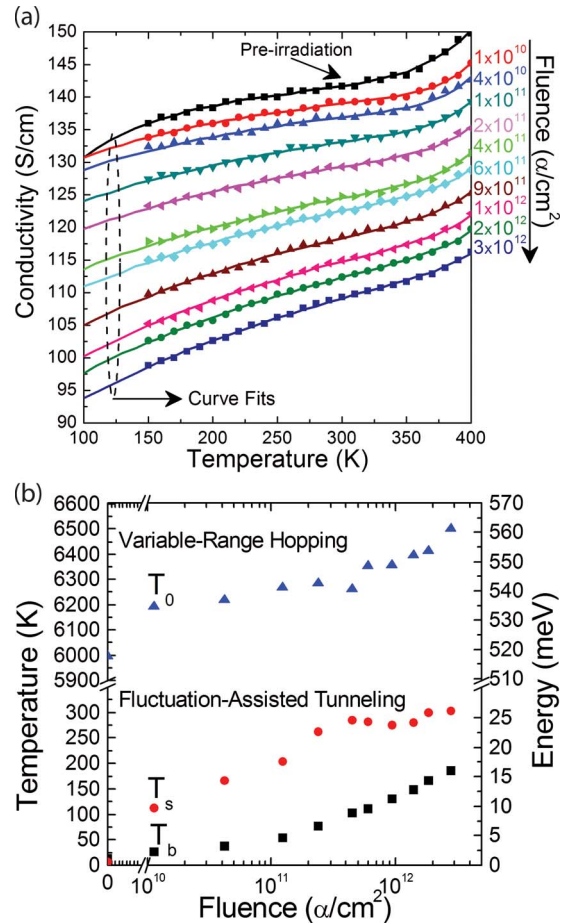


FIG. 2. (Color online) (a) The temperature-dependent SWCNT paper conductivity for increasing alpha-particle fluence measured *in situ* under a vacuum of $\sim 5 \times 10^{-6}$ Torr. The solid lines in the figure are least-squares curve fits of the data using Eq. (1). (b) Variation in [Eq. (1)] temperature curve fitting parameters as a function of alpha-particle fluence.

charging.¹² Above 350 K, a rapid increase in conductivity is observed, which may be attributed to a variable range hopping mechanism where conduction proceeds as phonon-assisted tunneling or as hopping between states within neighboring SWCNT/SWCNT bundles that are not necessarily located at equal energies.¹² Taken together, the temperature-dependent conductivity can be described with the following functional form:¹⁵

$$\sigma(T) = B \exp\left(-\frac{T_b}{T_s + T}\right) + H \exp\left[-\left(\frac{T_0}{T}\right)^\gamma\right]. \quad (1)$$

The geometrical fitting constants, B and H , are used to determine the relative contribution of the fluctuation assisted tunneling through barrier terms and the variable range hopping term, respectively, to the overall conductivity.¹² The fitting parameter, T_b , is related to the magnitude of the tunneling energy barrier, while the ratio, T_s/T_b , indicates the conductivity without thermal energy and therefore is related to the zero temperature conductivity. In the variable range hopping term, a value of $\gamma=1$ yielded the most consistent results and is indicative of electron transport by thermal excitation into a conduction band of extended states in a crystalline semiconductor at elevated temperatures.¹²

The variation in the fitting parameters, T_b , T_s , and T_0 , with alpha-particle fluence is plotted in Fig. 2(b). For each of these fits, B and H were assumed to be constant, while the temperature fitting parameters were allowed to vary. A gradual increase with alpha-particle fluence is observed in the values of all three parameters. The value of T_b increases with irradiation from 13 to 200 K, implying increasing barrier height, from 1.1 to 17.3 meV, for electronic tunneling between SWCNTs or SWCNT bundles with alpha-particle fluence. This increase may result from radiation-induced defects generated in the sidewalls disrupting the crystallinity of the SWCNTs and therefore reducing the wavefunction overlap between neighbors. Previously reported values of 22.5, 52, and 65 K have been identified as barrier T_b values, which are within the observed range for the current study.¹⁶ Initially, the T_s/T_b ratio was ~ 4.5 (after a fluence of 10^{10} alpha/cm²), and slowly reduces with increasing radiation, suggesting an increased zero temperature conductivity with the fluence. These changes indicate that conduction along the length of an individual SWCNT is hindered due to the localized defects necessitating the transport through higher barriers between SWCNTs in a bundle and neighboring bundles. The initial thermal energy barrier of $k_B T_0 = 520$ meV corresponds with the minimum bandgap energy in the distribution of laser-synthesized SWCNTs and is in agreement with the variable range hopping mechanism proceeding via thermalization or activation of electrons into excited states, allowing for more efficient tunneling to neighboring SWCNTs. The trend of increasing T_0 parameter with alpha-particle fluence indicates an increasing localization of electronic wavefunction resulting from radiation-induced defects in the SWCNTs. This increase indicates that variable range hopping is less effective after higher fluences, as evidenced by the continual reduction in high-temperature (> 350 K) conductivity increase as compared to the preirradiation case in Fig. 2(a). An increased localization can result from segmenting the SWCNT into regions of high conductivity separated by radiation-induced defects that reduce or eliminate transport along the SWCNT making hopping through higher energy barriers the newly formed lowest resistance path.

IV. RADIATION DAMAGE ANALYSIS AND DISCUSSION

Modeling the defect distribution generated by the alpha-particle irradiation is necessary for accurately assessing the radiation response. In particular, to study radiation damage effects on the electrical conductivity of a material, it is necessary to achieve uniform damage throughout the material since electronic transport is along the least resistive path (i.e., the path in the SWCNT paper that is least damaged if a nonuniform damage profile is generated). The isotropic nature of the alpha particles emitted from the ²¹⁰Po source used to irradiate the SWCNT paper results in a large percentage of particles that impact the paper with high incident angle. Therefore, many alpha particles will come to rest prior to escaping the film, thereby changing the amount of damage (i.e., number of defects) imparted per ion. This could lead to a nonuniform damage profile in the paper,¹⁵ thus obscuring

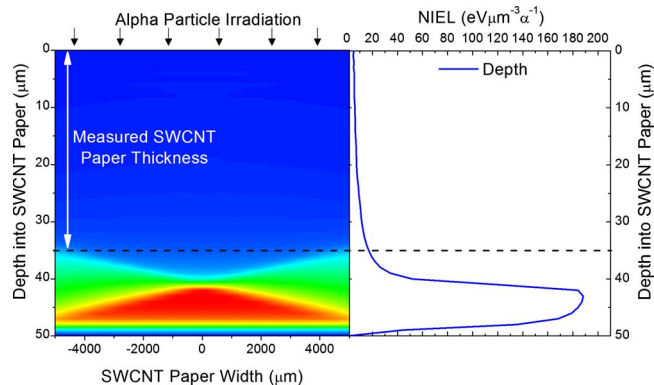


FIG. 3. (Color online) The NIEL profile of alpha particles incident with SWCNT paper (left), with the corresponding NIEL along a path down the midpoint of the SWCNT paper.

the true radiation response of the material. To assess the spatial distribution of damage created within the SWCNT paper from the alpha-particle irradiation, the nonionizing energy loss (NIEL) profile within the SWCNT paper was calculated using the geometry measured, with 16.9 eV as the threshold for carbon displacement in the SWCNT paper,⁶ 0.8 g/cm³ as the SWCNT paper density, 2.5 cm² circular area of alpha-particle source, and a 14 mm separation between the source and the SWCNT paper.¹⁷ Additionally, the thickness of the paper was simulated to be 50 μm so that the entire range of the alpha particles that are normally incident with the film would be completely stopped. The NIEL (for a particular particle and energy incident with a given material) is the rate of energy deposited within the SWCNT paper that results in the formation of displacement damage (i.e., SWCNT lattice defects). The results of the modeling are depicted in Fig. 3 where the NIEL profile (left) and the NIEL along the center axis of the SWCNT paper (right) are illustrated. This geometric configuration of the source and SWCNT paper irradiated *in vacuo* leads to a very favorable profile. In the range of the SWCNT paper (the top 35 μm), the damage is nearly uniform both as a function of depth and width. To arrive at an effective NIEL for the alpha particles emitted from the isotropic source, the NIEL profile was integrated over the full volume of the SWCNT paper to yield a value of 2.64 MeV cm² g⁻¹.

To compare the radiation response of SWCNT papers under alpha-particle radiation with studies performed on SWCNT papers using different irradiation particles, it is necessary to convert the particle fluences into a normalized unit since differences in range and total energy loss for the various particles make direct comparison meaningless. Normalizing the fluence based on NIEL is one approach that can be used to assess the effects of the different particles on the electrical conductivity of SWCNT papers in consistent units. For comparison with other reported data, the NIEL and range (in surface density units of g/cm²) of carbon ions, protons, and alpha particles (to compare with the isotropic irradiation conditions) in SWCNT papers were calculated using WINNIEL²¹⁸ and SRIM,¹⁹ respectively. A threshold energy for atomic displacement of carbon atoms in the SWCNT papers of 16.9 eV was used for all calculations.⁶ The NIEL and

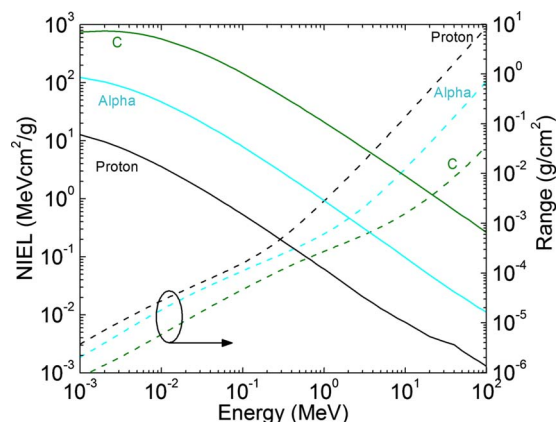


FIG. 4. (Color online) The NIEL and range of C, alpha particles, and protons stopping within a SWCNT paper. The NIEL values correspond to the solid lines and the left axis, while the range values are the dashed lines and correspond to the right axis. The range in units of centimeters can be determined by multiplying the values found in the figure by the density of the SWCNT paper or thin film.

range data are illustrated in Fig. 4. The NIEL for normally incident 4.2 MeV alpha particles can be obtained from this figure ($0.2 \text{ MeV cm}^2 \text{ g}^{-1}$) and is much lower than the effective NIEL ($2.64 \text{ MeV cm}^2 \text{ g}^{-1}$) obtained for the isotropic source because many alpha particles are slowed down and eventually come to rest at different depths within the paper in the isotropic case. It is also the case that lower energy particles have a larger NIEL value in a given material (see Fig. 4). For a given particle, the product of the NIEL and the particle fluence is referred to as the displacement damage dose (D_d), which is the total energy imparted to the structure going into displacement damage formation.²⁰ A plot of the conductivity (resistivity) as a function of D_d can subsequently be generated with many different irradiating particles with the total damage imparted to the SWCNT paper being identical for a given value of D_d , so long as the damage is uniform across the region of interest. Provided the damage caused by each irradiating particle causes the same type of defects, such a plot would lead to a single damage profile where the normalized conductivity (resistivity) versus D_d converge to a single line for all irradiating particles.²¹

Using the NIEL values from Fig. 4 for carbon ions and protons and the effective NIEL value for the isotropic alpha particle irradiation, the changes in electrical resistivity in SWCNT papers as a function of D_d for the three particles can be compared. Figure 5 shows the normalized resistivity values, at room temperature, for SWCNT papers irradiated with alpha particles (this study), 23 MeV carbon ions²² and 2 MeV protons.²³ Linear trend lines are plotted for the three data sets and the corresponding damage coefficients (i.e., the rate of change in normalized resistivity with respect to particle fluence) and NIEL values are provided in Table I. The rate of change in the damage coefficient as a function of NIEL provides a means to determine the dependence of defect production with energy loss per unit distance and is plotted for these particles in the inset of Fig. 5.²⁴ A nonlinear relationship (which can be approximated by a power-law relationship with an exponent of 1.94) for damage rate dependence on NIEL was found and indicates that increasing the

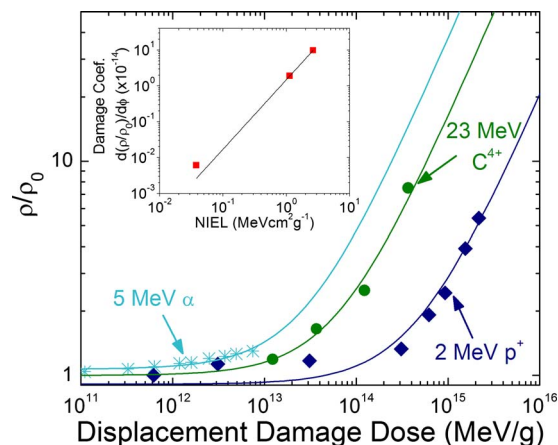


FIG. 5. (Color online) Variation in the SWCNT paper resistivity with displacement damage dose for various irradiating particles including 5 MeV alpha particles from an isotropic source, 23 MeV carbon atoms (Ref. 22), and 2 MeV protons (Ref. 23). Inset: damage coefficient variation with NIEL; the trend line is a power-law fit, $y = ax^b$, with $a = 1.5 \times 10^{-14}$ and $b = 1.94$.

rate (per unit length) of nonionizing energy deposition in SWCNT papers results in a comparably greater amount of reduction in the electronic transport. No such correlation is observed for the ionizing energy deposition since the linear energy transfer for 23 MeV C ions is greater than that of the 4.2 MeV alpha particles but the damage coefficient is less. Therefore, the quadratic dependence of the damage coefficient with NIEL implies that localized damage within a single SWCNT or a SWCNT bundle causes a larger disruption to the bulk SWCNT paper conductivity than distributed defects occurring in different SWCNT bundles within the paper.

Typical material properties (e.g., superconductor transition temperature²¹) and device characteristics (e.g., GaAs/Ge solar cell power output²¹ and GaAs/AlGaAs high electron mobility transistor-HEMT drain current²⁵) display a linear dependence of damage coefficient on NIEL for protons and ions, in contrast to the nearly quadratic dependence observed here in the SWCNT paper resistivity. In the aforementioned materials and devices, the parameters investigated were derived from the bulk properties of the material, or in the case of the HEMTs, the two dimensional confined electron-gas properties were altered. In contrast, conduction in SWCNT papers is largely one dimensional (1D), becoming bulk-like on the macroscopic scale due to the necessity to tunnel between neighboring SWCNT/SWCNT bundles for distances greater than the length of individual SWCNTs. At moderate temperatures (below 350 K), transport through the barriers

TABLE I. NIEL and damage coefficients for various particles in SWCNT papers.

Particle	NIEL ($\text{MeV cm}^2 \text{ g}^{-1}$)	Damage coefficient $d(\rho/\rho_0)/d\phi$
5 MeV alpha (Iso.)	2.64	9.79×10^{-14}
2 MeV proton	0.04	6.09×10^{-17}
23 MeV C ⁴⁺	1.13	1.89×10^{-14}

dominates the resistivity of the material and proceeds as fluctuation assisted tunneling. At elevated temperature, the effect of these barriers greatly reduces when variable range hopping begins to contribute. Distributed radiation damage (low NIEL) of the SWCNT paper results in small decreases in the paper transport (e.g., see proton data for $D_d < 5 \times 10^{14}$ in Fig. 5). At higher displacement damage doses, the concentration of defects is sufficiently large to disrupt the wavefunction overlap between neighboring SWCNT/SWCNT bundles and therefore yields an overall reduction in the SWCNT paper conductivity. In contrast, localized damage (high NIEL) causes much greater SWCNT damage, thus eliminating transport through individual SWCNTs at lower total displacement damage doses. This effectively segments the SWCNT, thereby disrupting the 1D transport along the nanotube length and forces electrons to tunnel through higher barriers (more resistance) to conduct throughout the paper. Therefore, the NIEL analysis indicates that the transport of SWCNT papers is still largely 1D, and it is the level of damage to these paths, or the degree of segmentation in the SWCNT/SWCNT bundles, that ultimately dictates the radiation response. This behavior should be fundamentally linked to the 1D nature of the material system, and therefore it is expected that other nanowire-based material composites will show similar radiation responses with deviations pertaining to both material aspect ratio and orientation.

V. CONCLUSION

The effects of ionizing radiation on the temperature-dependent electrical conductivity have been assessed *in situ* under a high vacuum environment. Irradiation of the SWCNT paper yielded a continual decrease in the total conductivity with increasing fluence. An analysis of the temperature-dependent conductivity as a function of alpha-particle irradiation indicates that the changes in the conductivity stem from increased barriers between adjacent SWCNTs and an increase in the electronic wavefunction localization. The displacement damage dose profile generated by the alpha-particle irradiation within the SWCNT paper was calculated and confirms that a uniform displacement damage dose (at the macroscopic level) was imparted to the paper. A comparison of the rate of change in resistivity for SWCNT papers irradiated with 23 MeV carbon ions and 2 MeV protons indicates a nonlinear dependence of resistivity increase in NIEL, which is distinctive from the linear response commonly observed in bulk semiconductors and superconductors. This result suggests that localized damage imparted to individual SWCNTs or SWCNT bundles causes more damage to the overall SWCNT paper conductivity than distributed point defects in the material under equivalent total displacement damage doses. Though bulk-like in many

aspects, the underlying 1D conducting nature of SWCNTs and SWCNT bundles can be observed in the radiation response of the material and is expected to be expressed for other bulk materials comprising high-aspect ratio nanostructures.

ACKNOWLEDGMENTS

This work was funded in part by the U.S. Department of Defense and in part by the U.S. Government. C.D.C. acknowledges postdoctoral funding from the National Research Council and is grateful to J.H. Warner, B.D. Weaver, and G.G. Jernigan for helpful discussions and for their review of the manuscript.

- ¹P. Avouris, Z. Chen, and V. Perebeinos, *Nat. Nanotechnol.* **2**, 605 (2007).
- ²D. Simien, J. A. Fagan, W. Luo, J. F. Douglas, and K. Migler, *ACS Nano* **2**, 1879–1884 (2008).
- ³E. S. Snow, F. K. Perkins, E. J. Houser, S. C. Badescu, and T. L. Reinecke, *Science* **307**, 1942 (2005).
- ⁴A. Tolvanen, G. Buchs, P. Ruffieux, P. Gröning, O. Gröning, and A. Krashenninnikov, *Phys. Rev. B* **79**, 125430 (2009).
- ⁵X. W. Tang, Y. Yang, W. Kim, Q. Wang, P. Qi, and H. Dai, *Phys. Med. Biol.* **50**, N23 (2005).
- ⁶B. W. Smith and D. E. Luzzi, *J. Appl. Phys.* **90**, 3509 (2001).
- ⁷W. K. Hong, C. Lee, D. Nepal, K. E. Geckeler, K. Shin, and T. Lee, *Nanotechnology* **17**, 5675 (2006).
- ⁸A. Kaiser, V. Skákalová, and S. Roth, *Physica E (Amsterdam)* **40**, 234 (2008).
- ⁹J. A. V. Pomoell, A. V. Krashenninnikov, K. Nordlund, and J. Keinonen, *J. Appl. Phys.* **96**, 2864 (2004).
- ¹⁰A. Krashenninnikov and K. Nordlund, *Nucl. Instrum. Methods Phys. Res. B* **216**, 355 (2004).
- ¹¹C. Mikó, M. Milas, J. W. Seo, E. Couteau, and N. Barišić, *Appl. Phys. Lett.* **83**, 4622 (2003).
- ¹²A. Kaiser, *Rep. Prog. Phys.* **64**, 1 (2001).
- ¹³B. J. Landi, C. D. Cress, C. M. Evans, and R. P. Raffaele, *Chem. Mater.* **17**, 6819 (2005).
- ¹⁴B. J. Landi, H. J. Ruf, C. M. Evans, C. D. Cress, and R. P. Raffaele, *J. Phys. Chem. B* **109**, 9952 (2005).
- ¹⁵V. Skákalová, A. Kaiser, Z. Osváth, G. Vértessy, L. Biró, and S. Roth, *Appl. Phys. A: Mater. Sci. Process.* **90**, 597 (2008).
- ¹⁶A. Kaiser, G. Düsberg, and S. Roth, *Phys. Rev. B* **57**, 1418 (1998).
- ¹⁷C. D. Cress, B. J. Landi, and R. P. Raffaele, *IEEE Trans. Nucl. Sci.* **55**, 1736 (2008).
- ¹⁸G. B. Gee, WINNIEL2 Version 2.0 Beta Test, available at <http://see.msfc.nasa.gov>.
- ¹⁹J. F. Ziegler, *Nucl. Instrum. Methods Phys. Res. B* **219**, 1027 (2004).
- ²⁰G. P. Summers, E. A. Burke, and M. A. Xapsos, *Radiat. Meas.* **24**, 1 (1995).
- ²¹S. R. Messenger, E. A. Burke, G. P. Summers, M. A. Xapsos, R. J. Walters, E. M. Jackson, and B. D. Weaver, *IEEE Trans. Nucl. Sci.* **46**, 1595 (1999).
- ²²V. Skakalova, A. B. Kaiser, U. Dettlaff, K. Arstila, A. Krashenninnikov, J. Keinonen, and S. Roth, *Phys. Status Solidi B* **245**, 2280 (2008).
- ²³B. D. Weaver, B. Landi, and R. Raffaele, *High Radiation Tolerance of Carbon Nanotube Matrices for Space Power Applications*, 2004 (AIAA, Reston, VA, 2004).
- ²⁴J. R. Srour, C. J. Marshall, and P. W. Marshall, *IEEE Trans. Nucl. Sci.* **50**, 653 (2003).
- ²⁵B. D. Weaver and E. M. Jackson, *Appl. Phys. Lett.* **80**, 2791 (2002).